Blessings of Dimensionality: Theoretical analysis of nearest-neighbor projected-distance methods for detecting interactions in high dimension

Bryan A. Dawkins[1], Trang T. Le[2] and Brett A. McKinney[1,3,*]

[1]Department of Mathematics, University of Tulsa, Tulsa, OK 74104, USA

[2] Department of Biostatistics, Epidemiology and Informatics, University of Pennsylvania, Philadelphia, PA 19104

[3]Tandy School of Computer Science, University of Tulsa, Tulsa, OK 74104, USA.

Abstract

It is commonly known that high-throughput data has many inherent statistical challenges, such as multiple testing, sparsity and over fitting. Collectively these challenges are known as the Curse of Dimensionality. Here we highlight an important Blessing of Dimensionality: the ability to identify interactions with nearest neighborhoods. We review nearest-neighbor concepts for finding interactions, and we derive important distribution moments for distance metrics in high dimensional spaces. We use these theoretical results and simulated data to offer recommendations for computational approaches to find nearest neighbors in high dimension. We discuss ways to maximize the blessings and minimize the curses of dimensionality to reliably identify interactions.

Author summary

Introduction

Relief-based methods identify interacting attributes as important by using nearest-neighbor information in higher dimensions (the "blessings of dimensionality"). Myopic methods, such as univariate tests, that do not account for information from higher dimensions, are susceptible to false negatives when there are interactions. For example in the plot of variable A versus C in a three-variable simulation (Fig. 1a), variable A appears to show no difference between cases and controls (the marginal group means are the same). However, A is actually simulated to have a strong differential correlation with B, conditioned on the outcome variable (Fig. 2b). Current Relief-based methods determine the importance of an attribute by computing the average difference of a target instance (X) and its nearest instance form the same class (Hit) projected onto the attribute A dimension ($d_{X,H}(A)$) subtracted from the projected difference of target X and its nearest instance from the opposite class (Miss) ($d_{X,M}(A)$). When the inequality $d_{X,M}(A) > d_{X,H}(A)$, it suggests that attribute A is useful for discriminating between cases and controls.

Fig 1. Imposters vs true neighbors in the presence of interactions with three variables. Scatter plot of simulated irrelevant Attribute C with a functional Attribute A **(a)**. None of the attributes has a main effect, but Attribute B and C interact through differential correlation **(b)**. Computing nearest neighbors with irrelevant attributes **(a)** or lower dimensions leads to imposter nearest neighbors and degrades the ability of Relief-based methods to identify interaction effects. Computing distances in only these two dimensions leads to an imposter false miss (FM) for the nearest neighbor from the opposite outcome class for target instance X. This imposter leads to attribute A predicting closer projected distances for misses than hits (H), which incorrectly indicates that A is a poor discriminator (yellow boxes in **(a)**). Computing nearest neighbors in higher dimensions **(c-d)** or with the correct interaction partner leads to imposter nearest neighbor (FM) being replaced by the true nearest miss neighbor (TM) for target instance X, which correctly leads to attribute A predicting closer projected distances for hits (H) than misses, which is an indication that attribute A is a good discriminator (yellow boxes **(b)**).

Relief-based methods use information from all attributes available to it (omnigenic) 16
to estimate an attribute's importance. However, if relevant higher-dimensional 17
information is not used, even Relief-based methods will miss the effect of A because 18
"imposter" neighbors will be used in the attribute estimate (False Miss (FM) in Fig. 1, 19
where $d_{X,FM}(A) < d_{X,H}(A)$). If one were to compute nearest neighbors in the A-C plane 20
(ignoring the B dimension), the nearest miss would be an imposter (FM), which leads to 21
a negative contribution to the importance score for A. One might call this C attribute a 22
type-I confounding attribute because it increases the chances of interacting attributes to 23
be false negatives. When nearest neighbors are calculated based on higher dimensions 24
with relevant information (Fig. 2c), it is clear that TM is closer to X than FM. The 25
imposter (FM) is replaced by the true nearest miss (TM) and attribute A correctly 26
shows a greater projected difference between misses than hits (Fig. 2d 27
$d_{X,TM}(A) > d_{X,H}(A)$), which is the signature of an important attribute. Univariate 28
methods still cannot find the importance of A unless the interaction is explicitly 29
modeled, but as long as functional variables A and B are in the space for nearest 30
neighbor calculations (Fig. 2c-d), imposters can be excluded and Relief-based methods 31
will find that A (and B) are important discriminators. 32

[Ideas: Relating the increasing k and myopic view to other distance-related method 33
such as MDS/t-SNE vs PCA - local vs global distance - capturing non-linear manifold 34
structure. 35
https://www.kdnuggets.com/2018/08/introduction-t-sne-python.html] 36

Using same interaction, increase background noise genes to see degrading of A and B 37
Relief importance because of curse of dimensionality (sparseness). 38
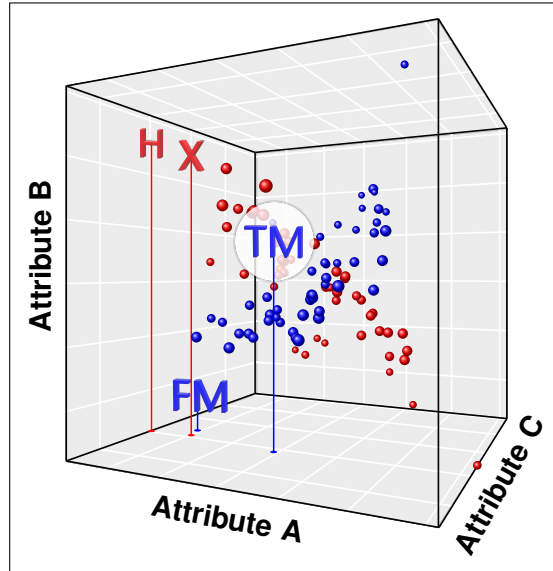
Fig 2. True neighbors

Fig 3. 3D AB view. Still working on this.

1 Neighborhood Methods

NPD methods rely on a neighborhood algorithm for feature selection. One may specify a fixed-k number of neighbors, an average radius SURF, a multiSURF radius that adapts for each instance [1], or a gene-wise adaptive-k.

2 Derivation of expected k for multiSURF neighborhoods

The multiSURF radius for an instance is the mean of its distances to all other instances subtracted by $\alpha = 1/2$ of the standard deviation of this mean. Previously we showed

Fig 4. 3D AC view. Still working on this.

empirically for balanced case-control datasets that a good constant-k approximation to the expected number of neighbors within the multiSURF radii is $k = m/6$ [2], where m is the number of samples. Here we derive a more exact theoretical mean that shows the mathematical connection between neighbor-finding methods. This fixed-k approximation to multi-SURF is independent of the type of data and the particular radii of each instance in the data.

2.1 Distribution of pairwise distances

Discuss Central Limit Theorem argument for the distribution being Gaussian. We can always say this is an assumption, but I think we can invoke the CLT. [I would be cautious here - TTL. We will be cautious invoking the CLT - BAM.]

Let $\mathcal{D}_X$ denote an arbitrary multivariate probability distribution with a corresponding univariate distribution $\mathcal{D}_x$. Consider $X = (X_1, X_2, \ldots, X_m)$ where $X_1, X_2, \ldots, X_m \overset{iid}{\sim} \mathcal{D}_X$. That is, each X_j is a random sample of length p such that $X_{ij} \overset{iid}{\sim} \mathcal{D}_x$. It is clear that X is a random data set of dimensions $p \times m$ such that $X_{ij} \overset{iid}{\sim} \mathcal{D}_x$ for $i = 1, 2, \ldots, p$ and $j = 1, 2, \ldots, m$.

Argument Outline

Manhattan

1. The Manhattan distance between instances j and k is a sum of magnitude differences $|X_{ij} - X_{ik}|$ for $i = 1, 2, \ldots, p$. That is

$$d(X_j, X_k) = D_{jk} = \sum_{i=1}^{p} |X_{ij} - X_{ik}|$$

2. The magnitude differences $y_i = |X_{ij} - X_{ik}| \overset{iid}{\sim} \mathcal{F}_y$.

3. The antecedent of the classical Central Limit Theorem is satisfied in (1) and (2).

4. The distribution of Manhattan distance between two fixed instances j and k is asymptotically normal by the classical Central Limit Theorem.

Euclidean

1. The Euclidean distance between instances j and k is the square root of the sum of squared differences $(X_{ij} - X_{ik})^2$ for $i = 1, 2, \ldots, p$. That is

$$d(X_j, X_k) = D_{jk} = \sqrt{\sum_{i=1}^{p} (X_{ij} - X_{ik})^2}$$

2. The squared differences $y_i = (X_{ij} - X_{ik})^2 \overset{iid}{\sim} \mathcal{F}_y$.

3. The antecedent of the classical Central Limit Theorem is satisfied in (1) and (2).

4. The distribution of the sum of squared differences between two fixed instances j and k is asymptotically normal by the classical Central Limit Theorem.

5. The square root function $f(x) = \sqrt{x}$ is a smooth functional transformation of the sum of squared differences.

6. Based on (4) and (5), the Delta Method implies that the Euclidean distance between two fixed instances j and k is asymptotically normal.

We may also want to show simulated distributions.

2.2 Predicted number of neighbors in the multiSURF alpha neighborhood

Regardless of the predictor data type (numeric or categorical), the distribution of the p predictors (uniform, Gaussian, or binomial), or the metric used to compute distances (Manhattan or Euclidean), the $m(m-1)/2$ pairwise distances in the p-dimensional space are well approximated by a normal distribution. An instance j is in the adaptive α-radius neighborhood of i ($j \in N_i^\alpha$) under the condition

$$D_{ij} \leq R_i^\alpha \implies j \in N_i^\alpha, \tag{1}$$

where the threshold radius for instance i is

$$R_i^\alpha = \bar{D}_i - \alpha \, \sigma_{\bar{D}_i} \tag{2}$$

and

$$\bar{D}_i = \frac{1}{m-1} \sum_{j \neq i} D_{ij}^{(\cdot)} \tag{3}$$

is the average of instance i's pairwise distances (using Eq. D Equation) with standard deviation $\sigma_{\bar{D}_i}$. MultiSURF uses $\alpha = 1/2$ [3].

The probability of the remaining $m - 1$ instances being inside the α-radius of instance i (R_i^α) can be viewed as $m - 1$ Bernoulli trials each with a probability of success q_α. Then the average average number of neighbors is given by

$$\bar{k}_\alpha = (m-1)q_\alpha, \tag{4}$$

from the mean of a binomial random variable. To calculate q_α, we assume the distribution of distances ($\{D_{ij}\}_{j \neq i}$) of neighbors of instance i is normal $N(\bar{D}_i, \sigma_{\bar{D}_i})$. Our empirical studies confirm a normal distribution and that it is robust to data type and metric. Extreme violations of independence of attributes (extreme correlations or

interactions) will cause the distribution to be right skewed, but this effect is difficult to observe in real data. Thus, for a Gaussian pairwise distance distribution, the probability q_α for one instance $j \neq i$ to be in the neighborhood of i ($j \in N_i^\alpha$) is given by the area under the mean-centered ($\bar{D}_i$) Gaussian from $-\infty$ to R_i^α. **show Gaussian plot illustration?** This integral can be written in terms of the error function (erf):

$$q_\alpha = \frac{1}{2}\left(1 - \text{erf}\left(\frac{\alpha}{\sqrt{2}}\right)\right). \tag{5}$$

And finally using Eqs. (4 and 5) we find

$$\bar{k}_\alpha = \left\lfloor \frac{m-1}{2}\left(1 - \text{erf}\left(\frac{\alpha}{\sqrt{2}}\right)\right)\right\rfloor, \tag{6}$$

where we apply the floor to ensure the number of neighbors is integer. For data with balanced hits and misses in standard fixed-k Relief, one divides this formula by 2. For multiSURF ($\alpha = 1/2$), this formula gives $\bar{k}_{1/2}^{\text{hit/miss}} = \frac{1}{2}\bar{k}_{1/2} = .154(m - 1)$, which is very close to our previous empirical estimate $m/6$. When we compare multiSURF neighborhood methods with fixed-k neighborhoods, we use $\bar{k}_{1/2}$. Using this $\alpha = 1/2$ value has been shown to give good performance for simulated data sets. However, the best value for α is likely data-specific and may be determined through nested cross-validation and other parameter tuning methods.

3 Derivation of means and standard deviations for metrics and data distributions

Table 1. Summary of asymptotic distance distributions for common data types. Metrics with subscripts M and E represent Manhattan and Euclidean, respectively. Metrics with superscript * represent the standard metric without attribute range normalization. The function $\Phi^{-1}(x)$ denotes the standard normal quantile function, where $x \in (0, 1)$.

Type	Mean	Variance
$\mathcal{N}(0,1) - \mathbf{d_M^*}$	$\dfrac{2p}{\sqrt{\pi}}$	$\dfrac{2p(\pi - 2)}{\pi}$
$\mathcal{N}(0,1) - \mathbf{d_M}$	$\boxed{\dfrac{p}{\sqrt{\pi}\mu(m)}}$ where $\quad \mu(m) = \dfrac{\log(\log(2))}{\Phi^{-1}\left(\frac{1}{m}\right)} - \Phi^{-1}\left(\frac{1}{m}\right)$	$\boxed{\dfrac{p(\pi - 2)}{2\pi\mu^2(m)}}$ where $\quad \mu(m) = \dfrac{\log(\log(2))}{\Phi^{-1}\left(\frac{1}{m}\right)} - \Phi^{-1}\left(\frac{1}{m}\right)$
$\mathcal{N}(0,1) - \mathbf{d_E^*}$	$\sqrt{2p - 1}$	1
$\mathcal{N}(0,1) - \mathbf{d_E}$	$\boxed{\dfrac{\sqrt{2p - 1}}{2\mu(m)}}$ where $\quad \mu(m) = \dfrac{\log(\log(2))}{\Phi^{-1}\left(\frac{1}{m}\right)} - \Phi^{-1}\left(\frac{1}{m}\right)$	$\boxed{\dfrac{2\log(m)}{\pi^2 + 12\mu^2(m)\log(m)}}$ where $\quad \mu(m) = \dfrac{\log(\log(2))}{\Phi^{-1}\left(\frac{1}{m}\right)} - \Phi^{-1}\left(\frac{1}{m}\right)$
$\mathcal{U}(0,1) - \mathbf{d_M^*}$	$\dfrac{p}{3}$	$\dfrac{p}{18}$
$\mathcal{U}(0,1) - \mathbf{d_M}$	$\dfrac{(m + 1)p}{3(m - 1)}$	$\dfrac{(m^3 - 18m^2 - 5m + 2)p}{18(m^3 + m^2 + 2)(m - 1)^2}$
$\mathcal{U}(0,1) - \mathbf{d_E^*}$	$\sqrt{\dfrac{p}{6} - \dfrac{7}{120}}$	$\dfrac{7}{120}$
$\mathcal{U}(0,1) - \mathbf{d_E}$	$\sqrt{\dfrac{p}{6} - \dfrac{7}{120}}\left(\dfrac{m + 1}{m - 1}\right)$	$\dfrac{7(m + 1)^2(m + 2)}{120(m^3 + m^2 + 2)}$

Table 2. Summary of asymptotic distance distributions for rs-fMRI and GWAS data. Metrics with superscript $*$ represent the standard metric without attribute range normalization. The function $\Phi^{-1}(x)$ denotes the standard normal quantile function, where $x \in (0,1)$.

Type	Mean	Variance
rs-fMRI $(\mathbf{d}_{\mathbf{ROI}}^{*})$	$\dfrac{2p(p-1)}{\sqrt{\pi(p-3)}}$	$\dfrac{4(\pi-2)p(p-1)}{\pi(p-3)}$
rs-fMRI $(\mathbf{d}_{\mathbf{ROI}})$	$\boxed{\dfrac{2p(p-1)}{\mu(m,p)\sqrt{\pi(p-3)}}}$ where $\quad \mu(m,p) = \dfrac{1}{\sqrt{p-3}}\Phi^{-1}\left(1 - \dfrac{1}{m(p-1)}\right)$	$\boxed{\dfrac{2[6(p-3)\mu^2(m,p)\log[m(p-1)](\pi-2) - \pi^2]p(p-1)}{\pi(p-3)\mu^2(m,p)(\pi^2 + 12(p-3)\mu^2(m,p)\log[m(p-1)])}}$ where $\quad \mu(m,p) = \dfrac{1}{\sqrt{p-3}}\Phi^{-1}\left(1 - \dfrac{1}{m(p-1)}\right)$
GWAS $(\mathbf{d}_{\mathbf{GM}})$	$\boxed{2\sum_{a=1}^{p} F(a)}$ where $F(a) = \left[2(1-f_a)^3 f_a + 2f_a^3(1-f_a) + (1-f_a)^2 f_a^2\right]$, and f_a is the probability of a minor allele at locus a.	$\boxed{2\sum_{a=1}^{p} F(a)[1 - 2F(a)]}$ where $F(a) = \left[2(1-f_a)^3 f_a + 2f_a^3(1-f_a) + (1-f_a)^2 f_a^2\right]$, and f_a is the probability of a minor allele at locus a.
GWAS $(\mathbf{d}_{\mathbf{AM}})$	$\boxed{2\sum_{a=1}^{p} F(a)}$ where $F(a) = \left[(1-f_a)^3 f_a + f_a^3(1-f_a) + (1-f_a)^2 f_a^2\right]$, and f_a is the probability of a minor allele at locus a.	$\boxed{\sum_{a=1}^{p}\left[G(a) - 4F^2(a)\right]}$ where $F(a) = \left[(1-f_a)^3 f_a + f_a^3(1-f_a) + f_a^3(1-f_a) + (1-f_a)^2 f_a^2\right]$, $G(a) = \left[(1-f_a)^3 f_a + f_a^3(1-f_a) + 2(1-f_a)^2 f_a^2\right]$, and f_a is the probability of a minor allele at locus a.
GWAS $(\mathbf{d}_{\mathbf{TiTv}})$	$\boxed{(\gamma_0 + \gamma_2 + 2\gamma_1)\sum_{a=1}^{p} F(a) + \left[\dfrac{3}{2}(\gamma_0 + \gamma_2) + 2\gamma_1\right]\sum_{a=1}^{p} G(a)}$ where $F(a) = \left[(1-f_a)^3 f_a + f_a^3(1-f_a)\right]$ and $G(a) = (1-f_a)^2 f_a^2$, f_a is the probability of a minor allele at locus a, and γ_0, γ_1, and γ_2 are probabilities of PuPu, PuPy, and PyPy, respectively, at locus a.	$\boxed{\left[\dfrac{1}{4}(\gamma_0 + \gamma_2) + \gamma_1\right]\sum_{a=1}^{p} F(a) + \left[\dfrac{9}{8}(\gamma_0 + \gamma_2) + 2\gamma_1\right]\sum_{a=1}^{p} G(a) + \sum_{a=1}^{p}\left[(\gamma_0 + \gamma_2 + 2\gamma_1)F(a) + \left[\dfrac{3}{2}(\gamma_0 + \gamma_2) + 2\gamma_1\right]G(a)\right]^2}$ where $F(a) = \left[(1-f_a)^3 f_a + f_a^3(1-f_a)\right]$ and $G(a) = (1-f_a)^2 f_a^2$, f_a is the probability of a minor allele at locus a, and γ_0, γ_1, and γ_2 are probabilities of PuPu, PuPy, and PyPy, respectively, at locus a.

4 Optimal neighborhood parameters for detecting effects

k or α. Balancing blessing and curse of dimensionality.

5 ICA?

Using same interaction, increase background noise genes to see degrading of A and B Relief importance because of curse of dimensionality (sparseness).

References

1. Ryan J. Urbanowicz, Randal S. Olson, Peter Schmitt, Melissa Meeker, and Jason H. Moore. Benchmarking relief-based feature selection methods for bioinformatics data mining. *Journal of Biomedical Informatics*, 85:168–188, 2018.

2. Trang T Le, Ryan J Urbanowicz, Jason H Moore, and Brett A McKinney. Statistical inference relief (stir) feature selection. *Bioinformatics*, page bty788, 2018.

3. Delaney Granizo-Mackenzie and Jason H Moore. Multiple threshold spatially uniform relieff for the genetic analysis of complex human diseases. In *European Conference on Evolutionary Computation, Machine Learning and Data Mining in Bioinformatics*, pages 1–10. Springer, 2013.